Reducing the uncertainty of laser straightness measurements via local saturation of imaging sensors

Stefan Hager, Ernst Csencsics, Han Woong Yoo, and Georg Schitter
Automation and Control Institute
Technische Universität Wien
Vienna, Austria

***Abstract*—This paper investigates causes of center detection errors in laser straightness measurements for precision positioning applications and proposes the calibration of these errors by utilizing the reversal method after reducing the center detection uncertainty. The uncertainty arising from unknown imaging errors, such as spatially varying pixel sensitivity and sensor pollution, is diminished by saturating the imaging sensor. The results demonstrate that the uncertainty can be reduced by a factor of 4.8, from 2.19 µm to 0.45 µm. This reduction justifies the application of the reversal method to calibrate the remaining center detection error, attributed to the shape of the laser beam cross-section in the image. Consequently, this enables straightness measurements with a repeatability of 0.34 µm.**

***Index Terms*—machine calibration, straightness measurement, spot center detection**

I. Introduction

Straightness measurement is commonly used for calibration of high-precision positioning machines which are built from several stacked linear actuators, e.g., coordinate measurement machines and CNC machines [1]–[3]. The deviations of the actuator trajectories from a straight line are quantified and the straightness and flatness profiles are defined, as depicted in Fig. 1.

Various measurement methods have been documented and discussed in literature [4], [5]. Interferometric measurements using a Wollaston prism yield results with sub-micrometer accuracy for measurement ranges of several meters [6], [7]. The method is rather expensive and the profile can only be determined in one direction (straightness or flatness). The straightness of linear stages is often evaluated by using a displacement probe and a solid, straight edge for reference [8]–[10]. This method cannot perform for actuators that are integrated in machines, as the reference is bulky and limited in portability. The taut wire method compares the straightness of the actuator against a metal wire [11]–[13]. The setting up of this method is time consuming. Laser straightness measurement is often used due to its simplicity and low expenses [14]–[16]. The target ,e.g., the mover of a linear stage, moves parallel to a collimated laser beam, which provides the straightness reference. The relative perpendicular motion between target and laser beam reveals the straightness profile of the actuator. The relative position of the laser beam is determined by a position sensitive device (PSD) which is mounted to the target and the trajectory of the laser beam on the PSD during the linear motion is recorded. Usually, the usage of analog PSDs (e.g., tetra-lateral PSDs, Quadrant Photo Diodes) is preferred due to their higher bandwidth [14], [17]. The performance of the straightness measurement is limited by the accuracy of the beam position detection. For analog PSDs, the beam shape cannot be monitored and the procedure of detecting the beam position cannot be modified, hence, errors can neither be recognized nor compensated [16]. CMOS imaging sensors, however, allow to capture the cross-section of the laser beam for potential error detection. The position of the laser beam is represented by the center of the laser spot in the captured image, which is determined by a center detection algorithm. In order to increase the accuracy of the measurement, calibration using the reversal method was proposed [15], [18]. However, the unknown error arising from imaging errors such as varying pixel sensitivity and sensor pollution can not be considered by this approach.

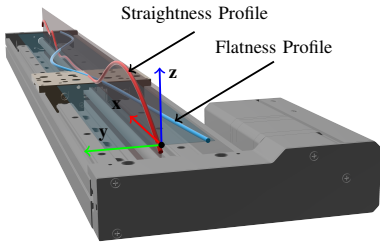

Fig. 1: Linear actuators are intended to perform linear motions. Deviations from these straight trajectories are known as straightness errors. In order to distinguish the profile of movement in x-y-plane from that in x-z-plane, the terms *straightness* and *flatness* are introduced.

The contribution of this paper is a novel approach for enhancing the precision of spot center detection via the deliberate saturation of imaging sensors. In the saturated regions, the impact of uncertainties induced by imaging errors can be suppressed at the expense of the systematic center detection error linked to the beam shape. This trade-off opens up opportunities for effective calibration to address and minimize the systematic error, thereby improving the overall accuracy of spot center detection in laser straightness measurements.

II. Problem Description

As outlined in Fig. 2, the linear actuator under test is aligned with the laser beam. The cross-section of the laser beam is

Affiliation: Christian Doppler Laboratory for Precision Measurements in Motion, Automation and Control Institute, TU Wien. Corresponding author: hager@acin.tuwien.ac.at

Pre-print version of the article: S. Hager, E. Csencsics, H.W. Yoo, and G. Schitter, "Reducing the uncertainty of laser straightness measurements via local saturation of imaging sensors," *2024 IEEE/ASME International Conference on Advanced Intelligent Mechatronics*, July 15th - 19th 2024, Boston, MA, USA, 2024.

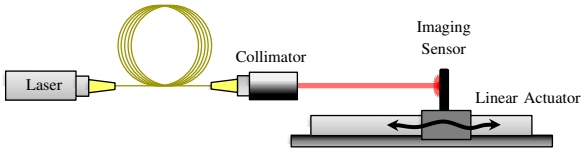

Fig. 2: Laser straightness measurement utilizes a fiber-coupled laser that is aligned with the direction of motion of the linear actuator. For straightness errors, the imaging sensor on the mover is displaced in orthogonal direction relative to the laser beam, what is visible in the position of the laser spot in the captured image.

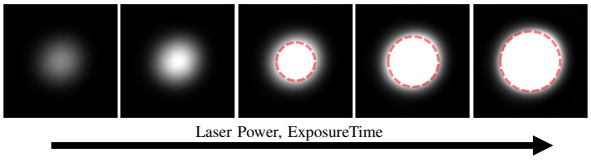

Fig. 3: For increasing laser power or exposure time, the image of the laser beam exhibits saturation in the center area of the spot (encircled in red). The diameter of the spot increases.

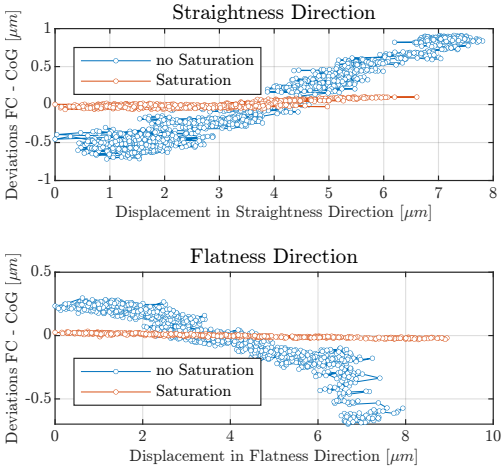

Fig. 4: The imaging sensor is displaced relative to the laser beam by the thermal expansion of the sensor mount. The perceived movements of the laser beam on the imaging sensor in straightness direction (upper plot) and flatness direction (lower plot) are detected by the center detection algorithms - Filter Correlation (FC) and Center of Gravity (CoG). However, the results differ from each other, indicating the presents of center detection errors. For increased laser power, the imaging sensor saturates and the results from different center detection algorithms show higher congruence.

captured by the imaging sensor on the mover and the spot center, representing the position of the spot in the image, needs to be determined. Monitoring the motion of the laser spot during linear movement reveals the straightness profile in straightness and flatness direction.

In order to measure the straightness of linear actuators with long travel range, the laser needs to exhibit sufficiently low divergence, requiring the beam diameter to be much bigger than the pixel size of the imaging sensor. Both, the laser power and the exposure time of the imaging sensor affect the image of the laser beam similarly. Figure 3 shows how the increase of the laser power or exposure time introduces local saturation of pixels that are in the center of the laser spot while increasing the diameter of the spot. Usually, saturation is avoided as it introduces non-linearities, which can impair the accuracy of the measurement [19], [20].

Several algorithms are applicable to find the center of the laser spot in the image. The evaluation of the center of gravity (CoG) gives the mean of the pixel coordinates weighted with the pixel intensity values [21]. Filter correlation (FC) determines the center of the spot by finding the location of the maximum in the cross-correlation function of the captured image and a Gaussian filter [22], that represents a model of the ideal cross-section of the laser beam. These two approaches for center detection yield different results, indicating the presents of center detection errors for at least one of the center detection algorithms. Figure 4 shows the results of a motivating experiment in which the deviations between the detected spot centers of both approaches are recorded while the laser spot is shifted by single micrometer in straightness or flatness direction, respectively. It is remarkable that the deviation is smaller with saturated images than with unsaturated images. This leads to the question, if the detected spot centers reliably represent the position of the laser spot in the captured image and if these centers can be actually taken as a straight reference. Further on, it is to investigate whether saturation can actually contribute to the reduction of the absolute center detection error without impairing the sensitivity of the measurement.

III. Method

The center detection error e_{CD} mainly depends on two circumstances, the position (u, v) of the laser beam on the imaging sensor and the distance d between collimator and sensor. In order to minimize the resulting measurement error, the aim is to reduce the unknown parts of the center detection error by introducing sensor saturation and cancel the known parts via calibration using the reversal method.

A. Spot Center Detection Error

Center detection errors limit the accuracy of straightness measurements. Two major contributors to this error can be determined. First, the shape of the laser beam itself is distorted due to interference, pollution of the collimator, static aberrations and divergence, introducing a component $\bar{e}_{CD}$ to the center detection error which is dependent on the distance d between the collimator and the imaging sensor, hence, $\bar{e}_{CD} = \bar{e}_{CD}(d)$. Second, the characteristics of the imaging sensor such as pixel shape, varying pixel sensitivity and dead pixels as well as pollution of the imaging sensor distort the image of the laser beam cross-section, adding a component $\tilde{e}_{CD}$ to the center detection error. This component depends on the position (u, v) of the laser spot in the captured image as well as on the shape and intensity of the spot, which is again dependent on the distance d between collimator and sensor. Hence, $\tilde{e}_{CD} = \tilde{e}_{CD}(d, u, v)$. While varying pixel sensitivity

Pre-print version of the article: S. Hager, E. Csencsics, H.W. Yoo, and G. Schitter, "Reducing the uncertainty of laser straightness measurements via local saturation of imaging sensors," *2024 IEEE/ASME International Conference on Advanced Intelligent Mechatronics*, July 15th - 19th 2024, Boston, MA, USA, 2024.

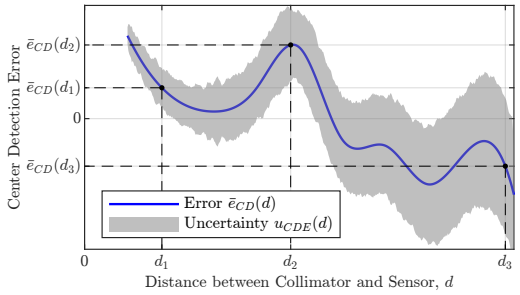

Fig. 5: The center detection error e_{CD} is composed of $\bar{e}_{CD}(d)$ due to the laser beam deformation and a measurement uncertainty $u_{CDE}(d)$, arising from the unknown contribution of $\tilde{e}_{CD}(d,u,v)$ due to the imaging sensor. Both, the error e_{CD} as well as its uncertainty $u_{CDE}(d)$, are expected to be dependent on the distance between collimator and sensor. The depicted plot shows an exemplary profile of the error e_{CD} for the purpose of visualization of the introduced variables.

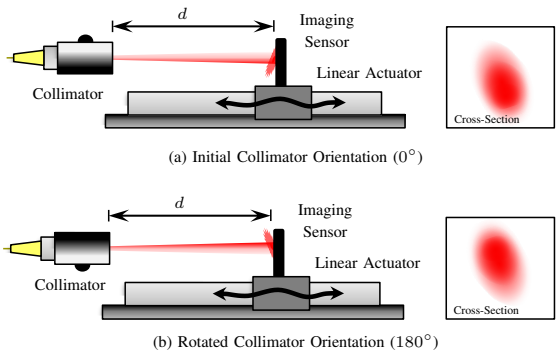

Fig. 6: For the reversal method, two measurements with different orientations of the collimator are conducted. The impact of the beam shape affects both measurements with opposite signs, allowing for its cancellation by calculating the mean over both measurement results.

is a bigger problem for smaller spots, sensor pollution has a major impact on the center detection of bigger spots, as the laser beam is partially shadowed or refracted by dust and streaks.

As consequence, the center detection error e_{CD} can be modeled as the sum of both contributors

$$e_{CD}(d,u,v) = \bar{e}_{CD}(d) + \tilde{e}_{CD}(d,u,v). \tag{1}$$

The second term due to the impact of the imaging sensor is intricate and remains unknown. It is classified as unknown systematic error and manifests in a measurement uncertainty $u_{CDE}(d)$ to $e_{CD}(d)$. The error $\bar{e}_{CD}(d)$, however, can be determined by investigating the deformation of the beam profile and how this impacts the center detection. As a result, the center detection error can be described by $\bar{e}_{CD}(d)$ with a remaining uncertainty via

$$e_{CD}(d) = \bar{e}_{CD}(d) \pm \underbrace{u_{CDE}(d)}_{\substack{\text{due to} \\ \text{unknown } \tilde{e}_{CD}}} . \tag{2}$$

Figure 5 sketches an example of the center detection error $e_{CD}(d)$ as a function of the distance d between collimator and sensor as well as the measurement uncertainty due to the unknown influence of the imaging sensor. For decreasing impact of the imaging sensor, the measurement uncertainty decreases until only $\bar{e}_{CD}(d)$ (plotted in blue) remains. For increasing distance d, the laser beam has a larger diameter due to the divergence, covering more of the imaging sensor area, increasing the sensors impact, hence, increasing the measurement uncertainty [23], [24]. In absence of other errors, $\bar{e}_{CD}(d)$ can be calibrated using the reversal method [15], making it a known systematic error.

B. Reversal Method

The reversal method is a commonly known calibration concept to determine repeatable measurement errors by conducting several measurements of the same sample so that the error impacts different measurement runs with different sign. In the case of straightness measurements, this method is applicable by rotating the collimator by 180° around it's optical axis between two measurement runs, such that the laser beam cross-section appears rotated on the imaging sensor (Fig. 6). As a result to this, the error $\bar{e}_{CD}(d)$, which arises from the beam deformation, impacts the measurement results $y(d)$ of both runs with opposite sign. In absence of other errors, the measurement results can be written as

$$y_{0°}(d) = s(d) + e_{CD}(d) \tag{3}$$
$$y_{180°}(d) = s(d) - e_{CD}(d), \tag{4}$$

with the straightness profile $s(d)$, arising from the straightness error of the linear actuator, the center detection error $e_{CD}(d)$ and the measurement results $y_{0°}(d)$ and $y_{180°}(d)$ for different orientations of the collimator. Due to alignment issues, the beam position on the imaging sensor differs for both measurement runs, hence, the error $\tilde{e}_{CD}(d,u,v)$ is different for both runs, indicated by $u_{CDE,1}(d)$ and $u_{CDE,2}(d)$. Considering these center detection uncertainties, the measurement results are composed of

$$y_{0°}(d) = s(d) + \bar{e}_{CD}(d) \pm u_{CDE,1}(d) \tag{5}$$
$$y_{180°}(d) = s(d) - \bar{e}_{CD}(d) \pm u_{CDE,2}(d). \tag{6}$$

From these measurements, the straightness profile $s(d)$ and the center detection error $\bar{e}_{CD}(d)$ can be determined via

$$s(d) = \frac{y_{0°}(d) + y_{180°}(d) \pm u_{CDE,1}(d) \pm u_{CDE,2}(d)}{2} \tag{7}$$
$$\bar{e}_{CD}(d) = \frac{y_{0°}(d) - y_{180°}(d) \pm u_{CDE,1}(d) \pm u_{CDE,2}(d)}{2}. \tag{8}$$

The uncertainties $u_{CDE,1}(d)$ and $u_{CDE,2}(d)$ are directly impacting the calibration and measurement result. Hence, it is important to reduce them as good as possible. This is achieved by reducing the impact of the imaging sensor characteristics and pollution by saturating the sensor pixels.

C. Uncertainty Reduction Strategy

The uncertainty in the center detection due to $\tilde{e}_{CD}$ is reduced by increasing the laser power and intentionally satu-

Pre-print version of the article: S. Hager, E. Csencsics, H.W. Yoo, and G. Schitter, "Reducing the uncertainty of laser straightness measurements via local saturation of imaging sensors," *2024 IEEE/ASME International Conference on Advanced Intelligent Mechatronics*, July 15th - 19th 2024, Boston, MA, USA, 2024.

rating the imaging sensor. The following discussion aims to establish a foundation for the principles of the uncertainty reduction for the spot center calculation using the CoG approach. For CoG, the center is determined via

$$\Delta CoG_u = \frac{\sum_{u\in U}\sum_{v\in V} uI_{uv}}{\sum_{u\in U}\sum_{v\in V} I_{uv}} \tag{9}$$

$$\Delta CoG_v = \frac{\sum_{u\in U}\sum_{v\in V} vI_{uv}}{\sum_{u\in U}\sum_{v\in V} I_{uv}}, \tag{10}$$

with the intensity I_{uv} of the laser beam cross-section in the position (u, v) in the sensor frame. Further on, the summation over all sensor pixel coordinates $u \in U$ and $v \in V$ is succinctly denoted using the symbol $\sum$. Even for a flawless imaging sensor, this calculation may give a result that differs from the laser beam axis, e.g., due to asymmetry of the laser beam in combination with the sensor's gamma value [23]. Hence, it is already subject to a center detection error $\bar{e}_{CD}$.

A practical imaging sensor, however, experiences imaging errors that modify the perceived intensity I_{uv} with an additional term E_{uv}. The resulting error in the spot center detection for the sensor's u-axis is given by

$$\Delta CoG_u = \tilde{e}_{CD} = \underbrace{\frac{\sum uI_{uv}}{\sum I_{uv}}}_{\substack{CoG_u \\ \text{for flawless sensor}}} - \underbrace{\frac{\sum u(I_{uv}-E_{uv})}{\sum (I_{uv}-E_{uv})}}_{\substack{CoG_u \\ \text{after imaging errors}}}. \tag{11}$$

The error E_{uv} is caused by different pixel sensitivities and shading due to sensor pollution. The first part is described by a mean-free random distribution across the entire sensor area. The last part reduces the intensity locally such that all contributions to the error have a positive sign. Due to this, the expected value of E_{uv} for any pixel can be assumed to be positive. Considering a sensor coordinate frame, who's origin coincides with the CoG before imaging errors, the term $\sum uI_{uv}$ evaluates to zero. Hence, the error can be described by

$$\Delta CoG_u = \tilde{e}_{CD} = \frac{\sum uE_{uv}}{\sum (I_{uv}-E_{uv})}. \tag{12}$$

Considering an axially symmetric beam, the CoG before imaging errors does not change due to saturation. First of all, for increasing laser power, the term $\sum I_{uv}$ increases, hence, the error $\tilde{e}_{CD}$ decreases. Second, the imaging error E_{uv} in the saturated regions is suppressed to zero, what reduces the expected value for E_{uv}, therefore $\sum E_{uv}$ and eventually $\tilde{e}_{CD}$. Due to the expected symmetry of the saturated area and the chosen coordinate frame such that $CoG_u = 0$, the term $\sum uE_{uv}$ will not be affected noteworthy. In conclusion, both, the increase of laser power as well as the saturation reduce the error $\tilde{e}_{CD}$, thereby diminishing the associated uncertainty u_{CDE}.

In other words, in the saturated regions, the pixel characteristics do not contribute to the spot center detection error. All pixel values are maximum and dust is not visible. Only the comparably small edge of the laser spot contributes to $\tilde{e}_{CD}$. Hence, the sensitivity of the center detection error to the position of the laser beam on the imaging sensor decreases, what equates to a reduction of the uncertainty of e_{CD}, enabling the utilization of the reversal method.

IV. Setup

The experimental setup consists of a laser with a wavelength of 635 nm which is coupled into a single-mode fiber with a collimator having a specified waist diameter of 0.8 mm. The laser beam cross-section is captured by a CMOS imaging sensor with a pixel size of 1.85 µm × 1.85 µm. The imaging sensor is mounted to the mover of a linear stage with a travel range of 500 mm. The repeatability of the linear stage is specified to be 1.5 µm. The distance between collimator and zero-position of the linear stage is 260 mm. An interferometer is used for displacement reference in straightness direction. Table I lists the components used in the setup.

TABLE I: Components used in the setup.

Component	***Manufacturer***	***Model***
Actuator	Zaber	LRT0500HL-BAE53CT10A
Imaging Sensor	The Imaging Source	DMM 37UX226-ML
Collimator	Thorlabs	F230FC-B
Fiber	Thorlabs	P1-630A-FC-1
Laser	Thorlabs	PL252
Interferometer	Attocube	IDS3010

V. Experiments and Results

In a first step, the uncertainty of the spot center detection is evaluated for different levels of saturation. The imaging sensor is displaced laterally and the spot center is detected via FC and CoG. For reference measurements, the displacement is monitored by an interferometer. The comparison of the position of the detected spot centers and the interferometer data yields $\tilde{e}_{CD}(d, u, v)$. From this, the uncertainty of the center detection can be determinted by calculating the standard deviation. The range of lateral displacement is 2 mm and 1000 equally spaced positions were recorded. Figure 7 shows the standard deviation of the center detection error for multiple saturation levels at a collimator-sensor distance of 720 mm, where the beam divergence is already well-noticeable. For increasing levels of saturation, the center detection improves and the uncertainty decreases until it reaches sub-pixel scale. The gain in precision is explained by the suppression of the impact of the sensor characteristics and pollution in the saturated areas. The CoG center detection algorithm shows better precision than the FC center detection algorithm, what may indicate that the chosen filter (Gaussian filter) does not represent the laser beam cross-section sufficiently good. The uncertainty can be reduced from 2.19 µm to 0.45 µm. For further experiments, the CoG algorithm is used.

This experiment gives evidence that the precision of the center detection can be increased by saturating the imaging sensor. The uncertainty u_{CDE} of the center detection due to

Pre-print version of the article: S. Hager, E. Csencsics, H.W. Yoo, and G. Schitter, "Reducing the uncertainty of laser straightness measurements via local saturation of imaging sensors," *2024 IEEE/ASME International Conference on Advanced Intelligent Mechatronics*, July 15th - 19th 2024, Boston, MA, USA, 2024.

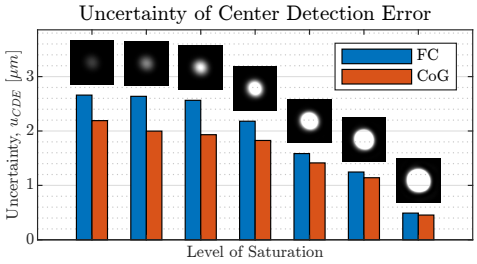

Fig. 7: Relative in-plane motion between the imaging sensor and the laser beam can be determined by evaluating the position of the spot center in the image. The comparison to an external interferometric reference reveals the precision of the center detection. The barplot shows the standard deviation (i.e., the uncertainty) of the center detection error for in-plane motion in a range of 2 mm for collimator-sensor distances of 720 mm.

the impact of the position of the laser beam on the imaging sensor is reduced significantly.

In the second step, the center detection error $e_{CD}(d)$ is determined using the reversal method. This gives the accuracy of the center detection. For this, the straightness measurement of the linear stage under test is performed several times with and without saturation on the imaging sensor and different collimator orientations of 0° and 180°. The center detection error $\bar{e}_{CD}(d)$ is obtained by (8). Figure 8 shows the determined center detection error $e_{CD}(d)$ for the saturated and the non-saturated case with uncertainty bands estimated from the previous experiment. The center detection error for the saturated case shows higher magnitudes, caused by the higher impact of the beam shape due to higher intensity values in the image and the increased spot size. Nevertheless, the significance is much higher due to the reduced uncertainty in $e_{CD}(d)$. The magnitude for the non-saturated case is hardly bigger than the uncertainty, such that the usage of the reversal method is not justified.

The knowledge about the center detection error $e_{CD}(d)$ enables system calibration by correcting measurement results for this error. As shown in (7) and (8), the uncertainty of the center detection error impacts the results for the calibrated straightness measurement in the same way as it impacts the result for the center detection error. Finally, Fig. 9 depicts the straightness and flatness profile of the linear stage under test together with the resulting $\pm 3\sigma$-uncertainty. For this actuator, the magnitude of the profiles is approximately 40 µm for straightness direction and 60 µm for flatness direction. The period of the ripple is 5 mm, what corresponds to the pitch of the driving spindle. The uncertainty for the non-saturated case is clearly visible, while the uncertainty for the saturated case is smaller by a factor of five. The standard deviation of the measurement repeatability for different calibration runs with saturation is 0.34 µm, what agrees well with the determined uncertainty of 0.45 µm from the first experiment.

In summary, the experiments prove that the introduction of sensor saturation reduces the uncertainty of the center detection error, which arises from the unknown impact of the imaging sensor. This enables the accurate use of the

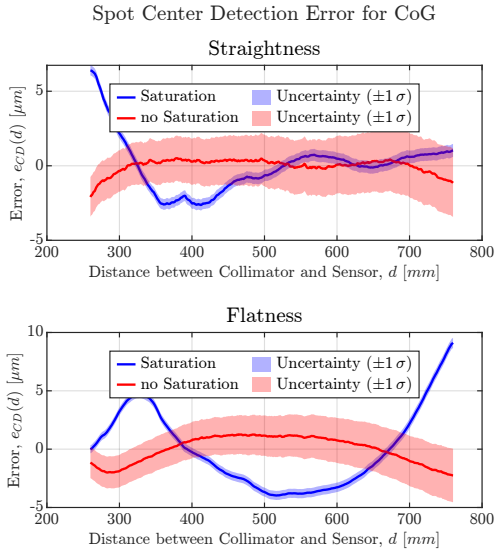

Fig. 8: The center detection error $e_{CD}(d) = \bar{e}_{CD}(d) \pm u_{CDE}(d)$ depending on the collimator-sensor distance d is determined using the reversal method, making it a known systematic error. While the magnitude of this error is larger for the saturated case, its significance is heightened due to the lower associated uncertainty.

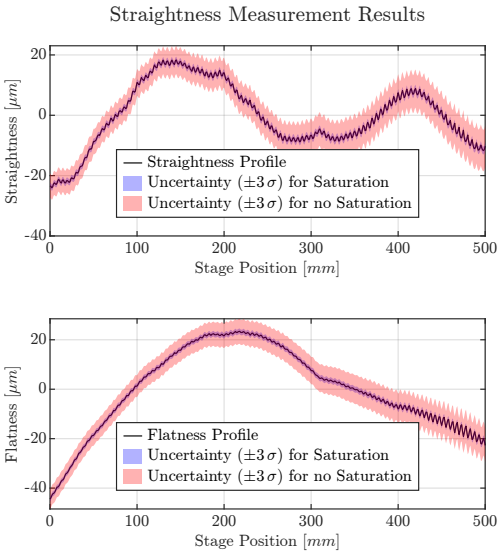

Fig. 9: The linear stage under test shows straightness errors with the magnitude of up to 60 µm. The uncertainty of the result without saturation is by a factor five bigger than for the saturated case.

Pre-print version of the article: S. Hager, E. Csencsics, H.W. Yoo, and G. Schitter, "Reducing the uncertainty of laser straightness measurements via local saturation of imaging sensors," *2024 IEEE/ASME International Conference on Advanced Intelligent Mechatronics*, July 15th - 19th 2024, Boston, MA, USA, 2024.

reversal method (cf. [15]) to determine the center detection error as a function of the collimator-sensor distance d with sub-micrometer precision.

VI. Conclusion

System calibration using the reversal method enables to correct the straightness measurement results for center detection errors, yielding more accurate results. In order to justify the use of the reversal method, it is important that the center detection uncertainty due to the impact of the position of the laser beam on the imaging sensor is small. It has been shown, that the introduction of sensor saturation reduces the uncertainty from $2.19\,\mu\text{m}$ to $0.45\,\mu\text{m}$. Due to the saturation and expansion of the spot in the image, the magnitude of the center detection error increases. However, calibration allows to correct for this known systematic error, yielding straightness measurements with sub-micrometer precision.

VII. Acknowledgment

The financial support by the Austrian Federal Ministry of Labour and Economy, the National Foundation for Research, Technology and Development and the Christian Doppler Research Association, and Micro-Epsilon Atensor GmbH and MICRO-EPSILON-MESSTECHNIK GmbH & Co.K.G. is gratefully acknowledged.

References

[1] W. Gao, S. Ibaraki, M. A. Donmez, D. Kono, J. Mayer, Y.-L. Chen, K. Szipka, A. Archenti, J.-M. Linares, and N. Suzuki, "Machine tool calibration: Measurement, modeling, and compensation of machine tool errors," *International Journal of Machine Tools and Manufacture*, vol. 187, p. 104017, Apr. 2023.

[2] H. Schwenke, W. Knapp, H. Haitjema, A. Weckenmann, R. Schmitt, and F. Delbressine, "Geometric error measurement and compensation of machines—An update," *CIRP Annals*, vol. 57, no. 2, pp. 660–675, 2008.

[3] H. Schwenke, R. Schmitt, P. Jatzkowski, and C. Warmann, "On-the-fly calibration of linear and rotary axes of machine tools and CMMs using a tracking interferometer," *CIRP Annals*, vol. 58, no. 1, pp. 477–480, 2009.

[4] K.-C. Fan, H.-Y. Wang, H.-W. Yang, and L.-M. Chen, "Techniques of multi-degree-of-freedom measurement on the linear motion errors of precision machines," *Advanced Optical Technologies*, vol. 3, pp. 375–386, Aug. 2014.

[5] W. Gao, S. Kim, H. Bosse, H. Haitjema, Y. Chen, X. Lu, W. Knapp, A. Weckenmann, W. Estler, and H. Kunzmann, "Measurement technologies for precision positioning," *CIRP Annals*, vol. 64, no. 2, pp. 773–796, 2015.

[6] B. Chen, W. Mao, Y. Lou, L. Yan, Z. Li, and Y. Yang, "Simultaneous measurement of the straightness error and its position using a modified Wollaston-prism-sensing homodyne interferometer," *Measurement Science and Technology*, vol. 31, p. 085004, Aug. 2020.

[7] Y. Lou, Z. Li, L. Yan, B. Chen, and J. Jiang, "A phase differential heterodyne interferometer for simultaneous measurement of straightness error and displacement," *Optics Communications*, vol. 497, p. 127195, Oct. 2021.

[8] A. Campbell, "Measurement of lathe z-slide straightness and parallelism using a flat land," *Precision Engineering*, vol. 17, no. 3, pp. 207–210, 1995.

[9] B. Di Giacomo, R. de Magalhães, and F. T. Paziani, "Reversal technique applied to the measurement of straightness errors," in *ABCM Symposium series in Mechatronics*, vol. 1, pp. 479–487, 2004.

[10] Z. qiang Yin and S. yi Li, "Exact straightness reconstruction for on-machine measuring precision workpiece," *Precision Engineering*, vol. 29, no. 4, pp. 456–466, 2005.

[11] O. Borisov, S. Fletcher, A. Longstaff, and A. Myers, "New low cost sensing head and taut wire method for automated straightness measurement of machine tool axes," *Optics and Lasers in Engineering*, vol. 51, pp. 978–985, Aug. 2013.

[12] O. Borisov, S. Fletcher, A. Longstaff, and A. Myers, "Performance evaluation of a new taut wire system for straightness measurement of machine tools," *Precision Engineering*, vol. 38, pp. 492–498, July 2014.

[13] J. G. Salsbury and R. J. Hocken, *Taut Wire Straightedge Reversal Artifact*, pp. 644–648. Boston, MA: Springer US, 2002.

[14] Y. Huang, K.-C. Fan, W. Sun, and S. Liu, "Low cost, compact 4-DOF measurement system with active compensation of beam angular drift error," *Optics Express*, vol. 26, p. 17185, June 2018.

[15] A. Küng, B. A. Bircher, and F. Meli, "Low-Cost 2D Index and Straightness Measurement System Based on a CMOS Image Sensor," *Sensors*, vol. 19, p. 5461, Dec. 2019.

[16] C. Kuang, E. Hong, Q. Feng, B. Zhang, and Z. Zhang, "A novel method to enhance the sensitivity for two-degrees-of-freedom straightness measurement," *Measurement Science and Technology*, vol. 18, pp. 3795–3800, Dec. 2007.

[17] X. Meng, S. Sun, X. Yan, F. Liu, L. Cao, Q. Wang, and Y. Sun, "Six-Degree-of-Freedom Posture Measurement Technologies Using Position Sensitive Detectors (PSDs): State of the Art," *Micromachines*, vol. 13, p. 1903, Nov. 2022.

[18] C. J. Evans, R. J. Hocken, and W. T. Estler, "Self-Calibration: Reversal, Redundancy, Error Separation, and 'Absolute Testing'," *CIRP Annals*, vol. 45, no. 2, pp. 617–634, 1996.

[19] X. Wei, J. Xu, J. Li, J. Yan, and G. Zhang, "S-curve centroiding error correction for star sensor," *Acta Astronautica*, vol. 99, pp. 231–241, June 2014.

[20] P. Zhou, X. Wang, Q. Huang, and C. Ma, "Laser spot center detection based on improved circled fitting algorithm," in *2018 2nd IEEE Advanced Information Management,Communicates,Electronic and Automation Control Conference (IMCEC)*, pp. 316–319, 2018.

[21] Z. Jiang, S. Gong, and Y. Dai, "Monte-carlo analysis of centroid detected accuracy for wavefront sensor," *Optics & Laser Technology*, vol. 37, no. 7, pp. 541–546, 2005.

[22] R. Szeliski, *Computer Vision: Algorithms and Applications*. Berlin, Heidelberg: Springer-Verlag, 1st ed., 2010.

[23] A. M. Nightingale and S. V. Gordeyev, "Shack-Hartmann wavefront sensor image analysis: a comparison of centroiding methods and image-processing techniques," *Optical Engineering*, vol. 52, no. 7, p. 071413, 2013.

[24] M. Dusek, K. Polak, J.-C. Gayde, M. Sulc, D. Mergelkuhl, and W. G. Niewiem, "Detection of structured laser beam centroid and its use for alignment," tech. rep., CERN, Geneva, 2022.

Pre-print version of the article: S. Hager, E. Csencsics, H.W. Yoo, and G. Schitter, "Reducing the uncertainty of laser straightness measurements via local saturation of imaging sensors," *2024 IEEE/ASME International Conference on Advanced Intelligent Mechatronics*, July 15th - 19th 2024, Boston, MA, USA, 2024.